OPEN

PRS GLOBAL OPEN

ORIGINAL ARTICLE
Research

# Tissue Expander–associated T Cells: Relevance to Breast Implant–associated Anaplastic Large-cell Lymphoma

Ichiro Shiokawa, MD*
Takuya Sato, MS†
Youichi Ogawa, MD, PhD*†
Yuka Nagasaka, MD*
Aoha Ishikawa, MD*
Shinji Shimada, MD, PhD†
Tatsuyoshi Kawamura, MD, PhD†
Akira Momosawa, MD, PhD*

**Background:** The generation of breast implant–associated anaplastic large-cell lymphoma (BIA-ALCL) is closely associated with textured implants. The phenotype of BIA-ALCL cells is well examined, but its cell of origin remains unknown. Here we investigate what types of T cells are recruited and differentiated in the surrounding capsules and tissues as a consequence of continuous contact with a textured surface.
**Methods:** Capsule and pericapsule tissues were recovered from patients who had textured or smooth tissue expanders (TEs). These samples were enzymatically digested, and T cells in the samples were analyzed using flow cytometry. Peripheral blood mononuclear cells from the same donors were utilized as a control.
**Results:** Effector memory $CD4^+$ T cells predominantly infiltrated capsules and tissues without apparent differences between textured and smooth TEs. In these effector memory $CD4^+$ T cells, $CD4^+$ resident memory T cells were generated by smooth TEs but not by textured TEs. However, *TNFRSF8/CD30* mRNA expression is higher in the $CD69^-$ effector memory $CD4^+$ T cells than in the $CD69^+$ ones.
**Conclusion:** Textured and smooth TEs differentially recruit and/or differentiate T cells in situ. *(Plast Reconstr Surg Glob Open 2022;10:e4148; doi: 10.1097/GOX.0000000000004148; Published online 23 March 2022.)*

## INTRODUCTION

The first case of breast-implant–associated anaplastic large-cell lymphoma (BIA-ALCL) was reported in 1997.[1] Thereafter, additional cases have been reported worldwide. The World Health Organization recognized BIA-ALCL as an entity distinct from other ALCLs in 2016.[2] Accumulating evidence has suggested that textured implants are closely associated with the pathomechanisms of BIA-ALCL,[3,4] and the US Food and Drug Administration issued a recall of Allergan Natrelle BIOCELL-textured implants and tissue expanders (TEs).[5] This incident was a great concern for patients who need a breast reconstruction. The BIOCELL surface is composed of irregular silicone projections and indentations with a variable pore size to promote tissue ingrowth and to prevent the circumferential linear fibrosis associated with capsular contracture around smooth silicone surfaces.[6] This macrotextured surface was beneficial for patients due to its low incidence of capsular contracture and prevention of malposition and rotation of implants by its adhesive effect on capsular tissue.[7,8]

BIA-ALCL is a T-cell neoplasm characterized by the clonal proliferation of large anaplastic cells, which phenotypically express CD30 but do not express anaplastic lymphoma kinase (ALK). However, the pathogenesis and pathomechanism of BIA-ALCL remains unclear,[9] and the origin of BIA-ALCL has not been extensively studied. Here we determined what types of T cells were recruited and differentiated in the surrounding capsules and tissues as a consequence of continuous contact with a textured surface. To this end, we characterized the T-cell phenotype in the capsules and tissues from patients who had macrotextured Natrelle 133 TE, which was recalled together with textured breast implants.

*From the *Department of Plastic Surgery Faculty of Medicine, University of Yamanashi, Yamanashi, Japan and †Department of Dermatology, Faculty of Medicine, University of Yamanashi, Yamanashi, Japan.*

*Received for publication November 8, 2021; accepted December 14, 2021.*

*Drs. Shiokawa and Sato contributed equally to this work.*



DOI: 10.1097/GOX.0000000000004148

**Disclosure:** *The authors have no financial interest in relation to the content of this article.*

Related Digital Media are available in the full-text version of the article on www.PRSGlobalOpen.com.

## MATERIALS AND METHODS

### Patients

Female patients who underwent TE removal for breast reconstruction between March 2020 and May 2021 were enrolled in this study. Patients with symptoms during TE implantation time were excluded. Patient demographic data are summarized in Supplemental Digital Content 1. (**See table, Supplemental Digital Content 1,** which displays the patient demographic data. **http://links.lww.com/PRSGO/B947**.)

### Sources of Tissues and Ethical Approval

The institutional review board of the university hospital (University of Yamanashi, Yamanashi, Japan) approved the acquisition of human tissues, and informed consent was obtained from all donors. Capsules, together with adjacent tissues surrounding TEs, were resected upon operation of TE removal. Peripheral blood was also taken from the same donors.

### Tissue Processing

The samples were washed with sterile cold PBS (Gibco, Dublin, Ireland) immediately following surgery. Subcutaneous fat was thoroughly removed. Pericapsule tissues were also removed from capsules by trimming with forceps (Fig. 1). These capsules and pericapsule tissues were used as samples. RPMI 1640 (Invitrogen Life Technologies, Carlsbad, Calif.) containing 10% FBS (Biowest, Nuaillé, France) and Anti-Anti (1:100; Gibco, Dublin, Ireland) without additional exogenous cytokines was utilized as a culture medium. Samples were placed in RPMI 1640 (Invitrogen Life Technologies, Carlsbad, Calif.)

### Takeaways

**Question:** What types of T cells are recruited and differentiated in the surrounding capsules and tissues as a consequence of continuous contact with textured or smooth implants?

**Findings:** Effector memory $CD4^+$ T cells predominantly infiltrated capsules and tissues without apparent differences between textured and smooth tissue expanders (TEs). In these effector memory $CD4^+$ T cells, $CD4^+$ resident memory T cells were generated by smooth TEs but not by textured TEs.

**Meaning:** Textured and smooth TEs differentially recruit and/or differentiate T cells in situ.

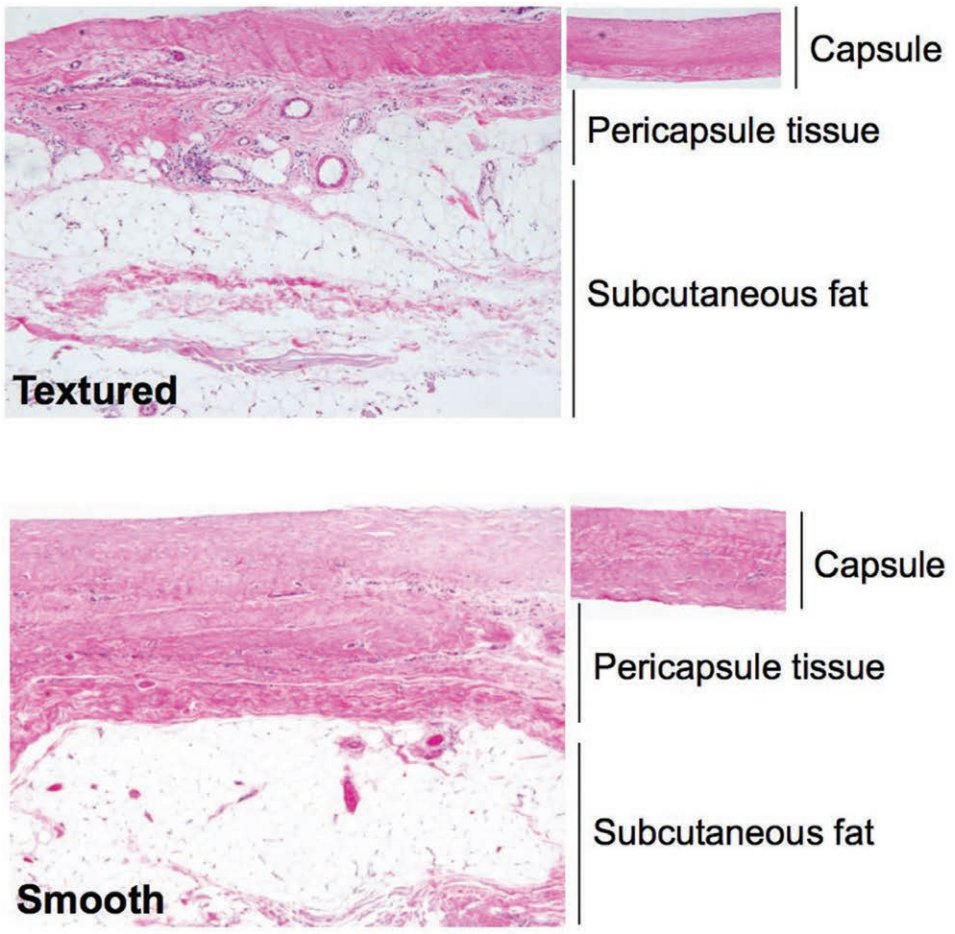


**Fig. 1.** Hematoxylin–eosin staining of capsules together with adjacent tissues surrounding textured TE and smooth TE.

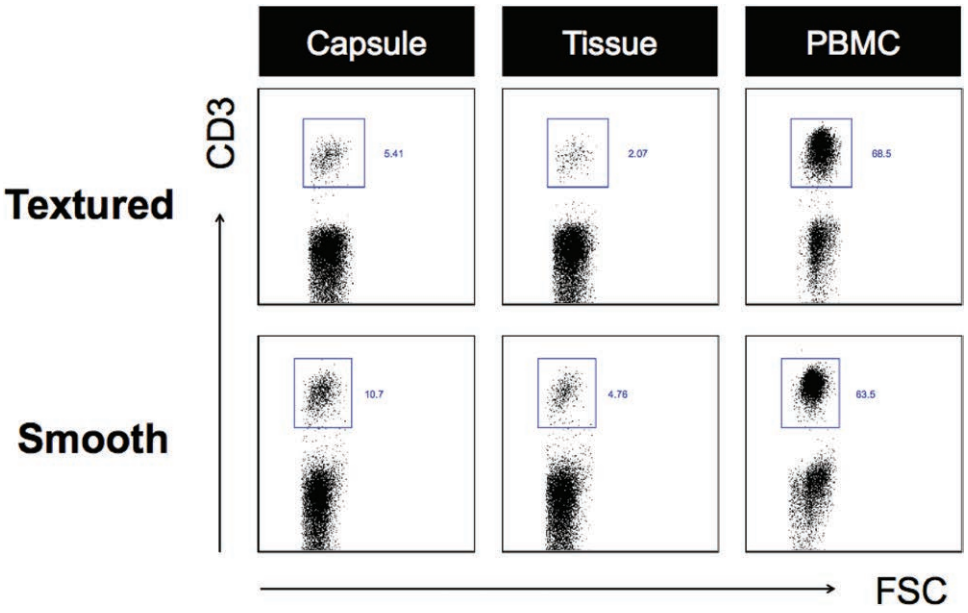


**Fig. 2.** Representative CD3 positivity in the indicated samples from textured and smooth TEs.

containing 200 U/mL collagenase type IV (Worthington, Lakewood, N.J.) and 0.05% DNaseI (Sigma-Aldrich, St. Louis, Mo.) for 120 min at 37°C. To generate single-cell suspensions, these pieces were aspirated with a 50-cm$^3$ syringe up and down 10 times. The sample was then filtered three times through a sterile mesh. In some experiments, debris was excluded using lympholyte-H cell separation medium (Cedarlane, Ontario, Canada) according to the manufacturer's instructions.

**Flow Cytometry**

The following monoclonal antibodies (mAbs) were used in this study: anti-CD3 (clone: HIT3a), anti-CD4 (clone: OKT-4), anti-CD8a (clone: HIT8a), anti-CD45RO (clone: UCHL1), anti-CD62L (clone: DREG-56), anti-CCR7 (clone: G043H7), anti-CD69 (clone: FN50), and anti-CD103 (clone: Ber-ACT8). These mAbs were purchased from BioLegend (San Diego, Calif.). Single-cell suspensions were incubated with mAbs for 30 min at 4°C and then washed twice in staining

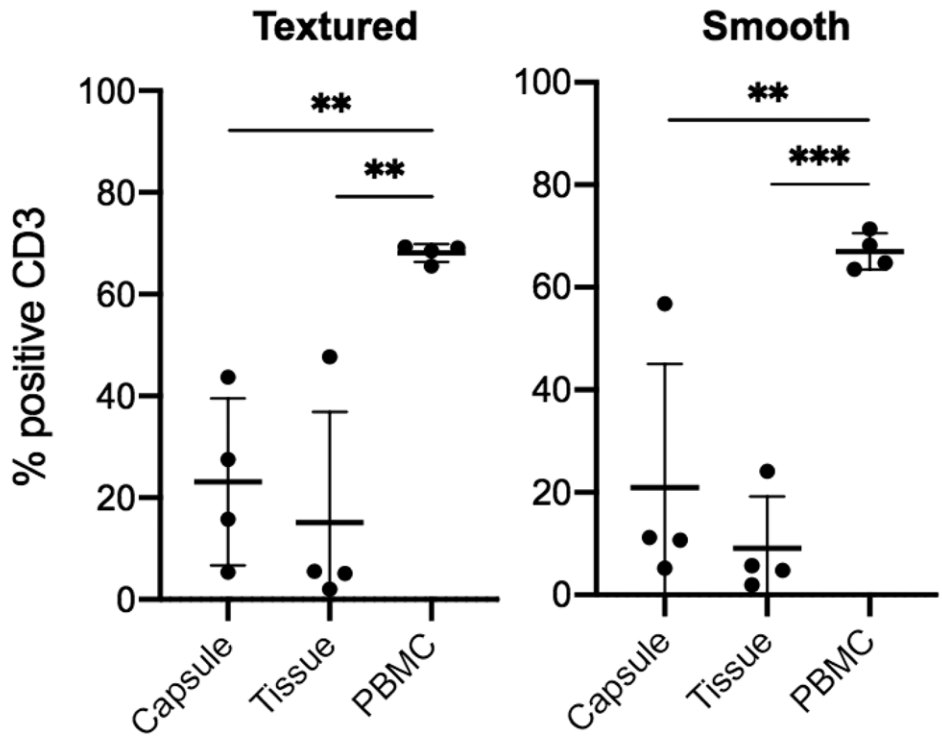


**Fig. 3.** A summary of CD3 positivity from four different donors.

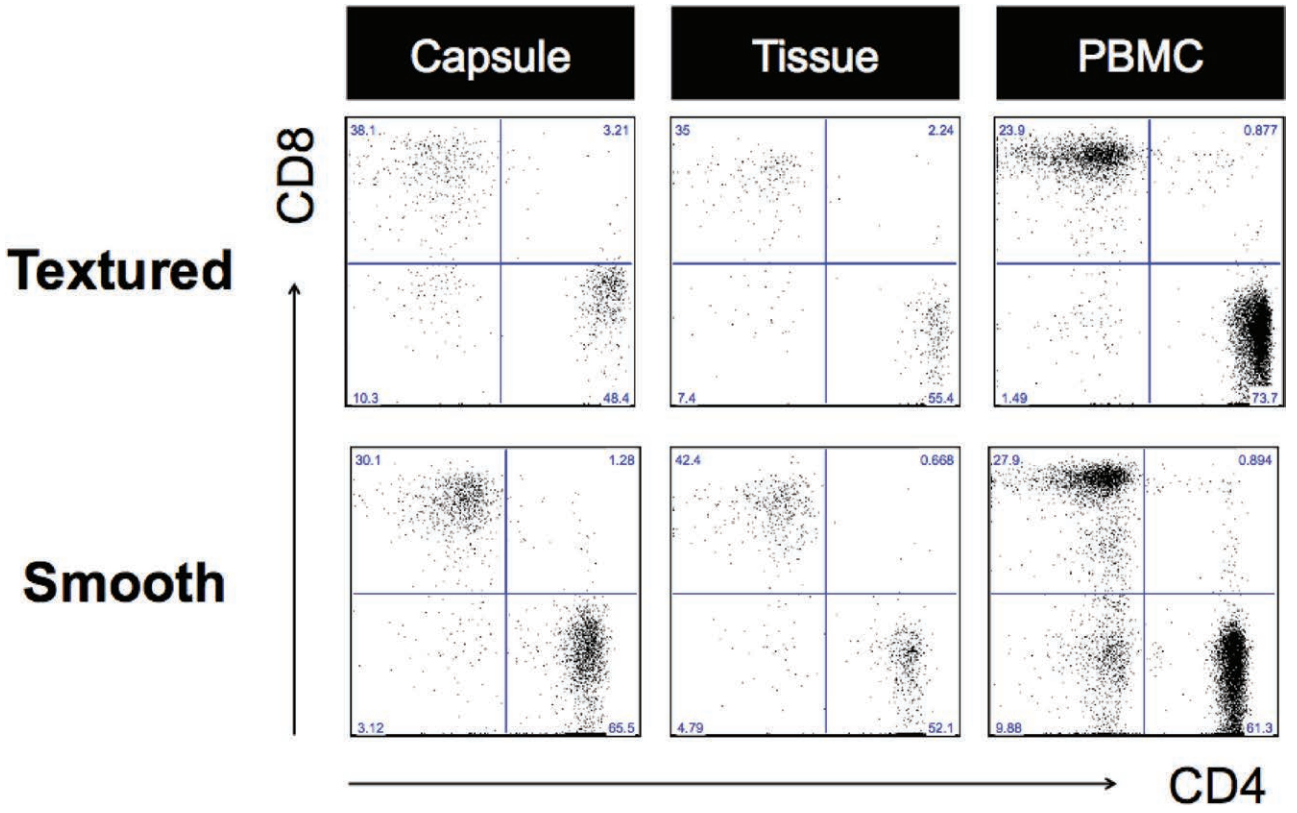


**Fig. 4.** Representative CD4 and CD8 positivity in the CD3-positive cells of the indicated samples from textured and smooth TEs.

buffer and examined using FACS Caliber (BD Biosciences, Franklin Lakes, N.J.). Dead cells were labeled by propidium iodide (Sigma-Aldrich, St. Louis, Mo.). Data were analyzed using the FlowJo software (FlowJo, LLC, Ashland, Oreg.).

**Quantitative PCR**

$CD3^+CD4^+CD69^-$ and $CD3^+CD4^+CD69^+$ T cells were isolated from five capsules of textured-TE donors as follows: $CD3^+CD4^+$ T cells were isolated using $CD4^+$ T Cell Isolation Kit (Miltenyi Biotec GmbH, Bergisch Gladbach, Germany) from single-cell suspensions of capsules of textured TE. These $CD3^+CD4^+$ T cells were incubated with FITC-conjugated anti-human CD69 mAbs (BioLegend, San Diego, Calif.) for 30 min at 4°C. After washing, Anti-FITC MicroBeads (Miltenyi Biotec GmbH, Bergisch Gladbach, Germany) were added, and then

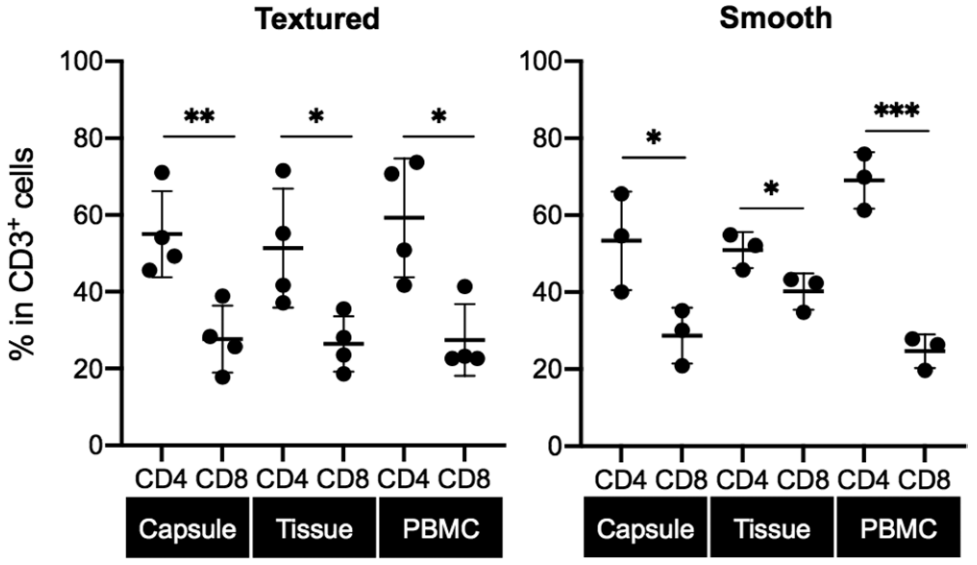


**Fig. 5.** A summary of CD4 and CD8 positivity from four different textured TE donors and three different smooth TE donors.

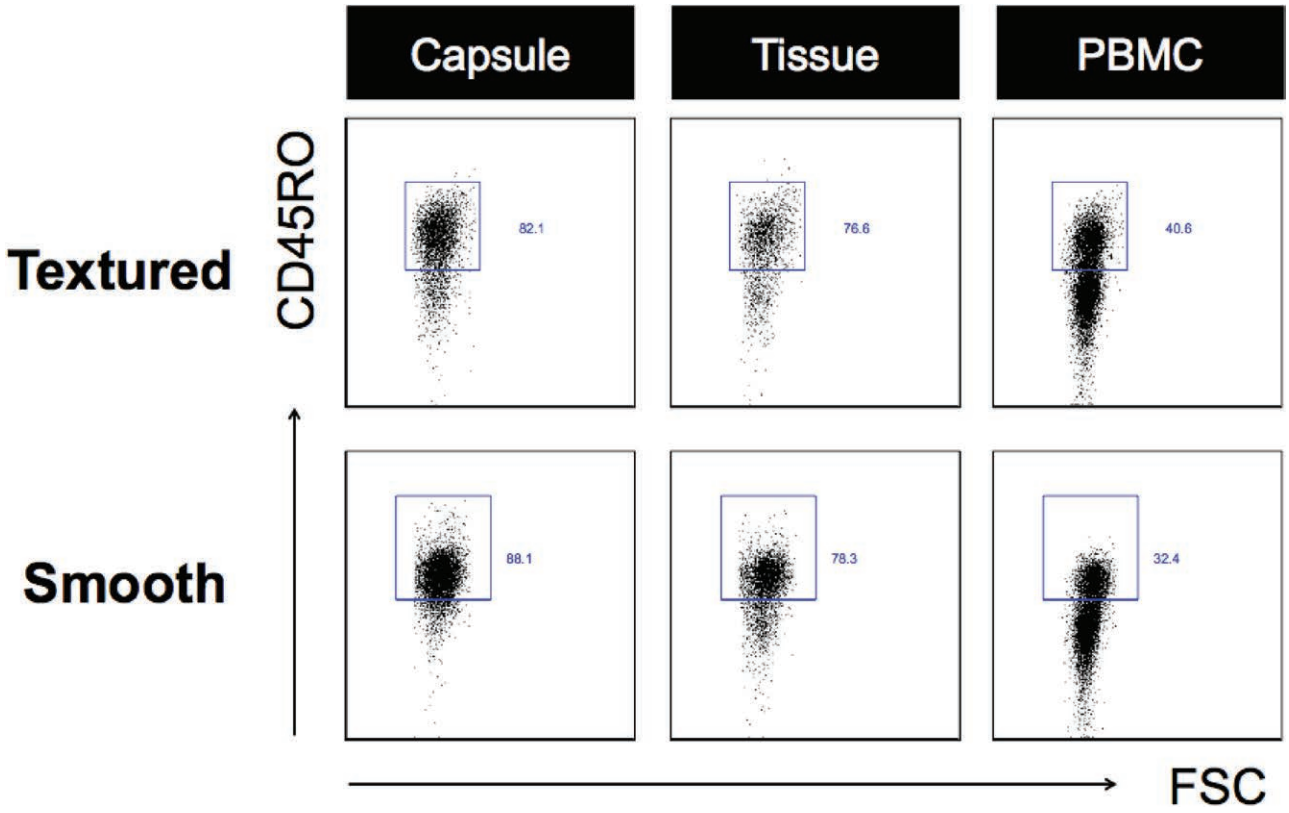


**Fig. 6.** Representative CD45RO positivity in the CD3-positive cells of the indicated samples from textured and smooth TEs.

$CD3^+CD4^+CD69^-$ and $CD3^+CD4^+CD69^+$ T cells were magnetically separated.

Total RNA was extracted using QIAzol Lysis Reagent (Qiagen, Hilden, Germany) and RNeasy Plus Universal Mini kit (Qiagen, Hilden, Germany) per the manufacturer's instructions. Reverse transcription was performed using ReverTra Ace qPCR RT Kit (Toyobo, Ohtsu, Japan) per the manufacturer's instructions. mRNA levels were determined using commercially available primer/probe sets (TaqMan Gene Expression Assay: Applied Biosystems, Foster City, Calif.) and the AB7500 real-time PCR system (Applied Biosystems, Foster City, Calif.). The amount of target gene mRNA obtained using real-time PCR was normalized against the amount of housekeeping control gene (*ACTB*) mRNA. A human CD30 primer was designed by Takara (Kyoto, Japan).

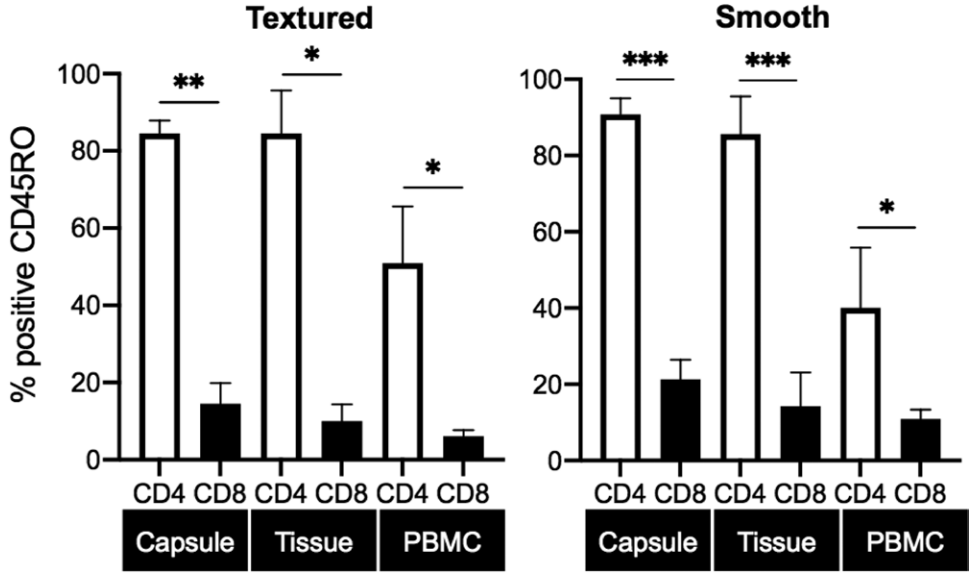


**Fig. 7.** A summary of CD45RO positivity from three different donors. $^*P < 0.05$, $^{**}P < 0.01$, and $^{***}P < 0.001$ (Student *t* test).

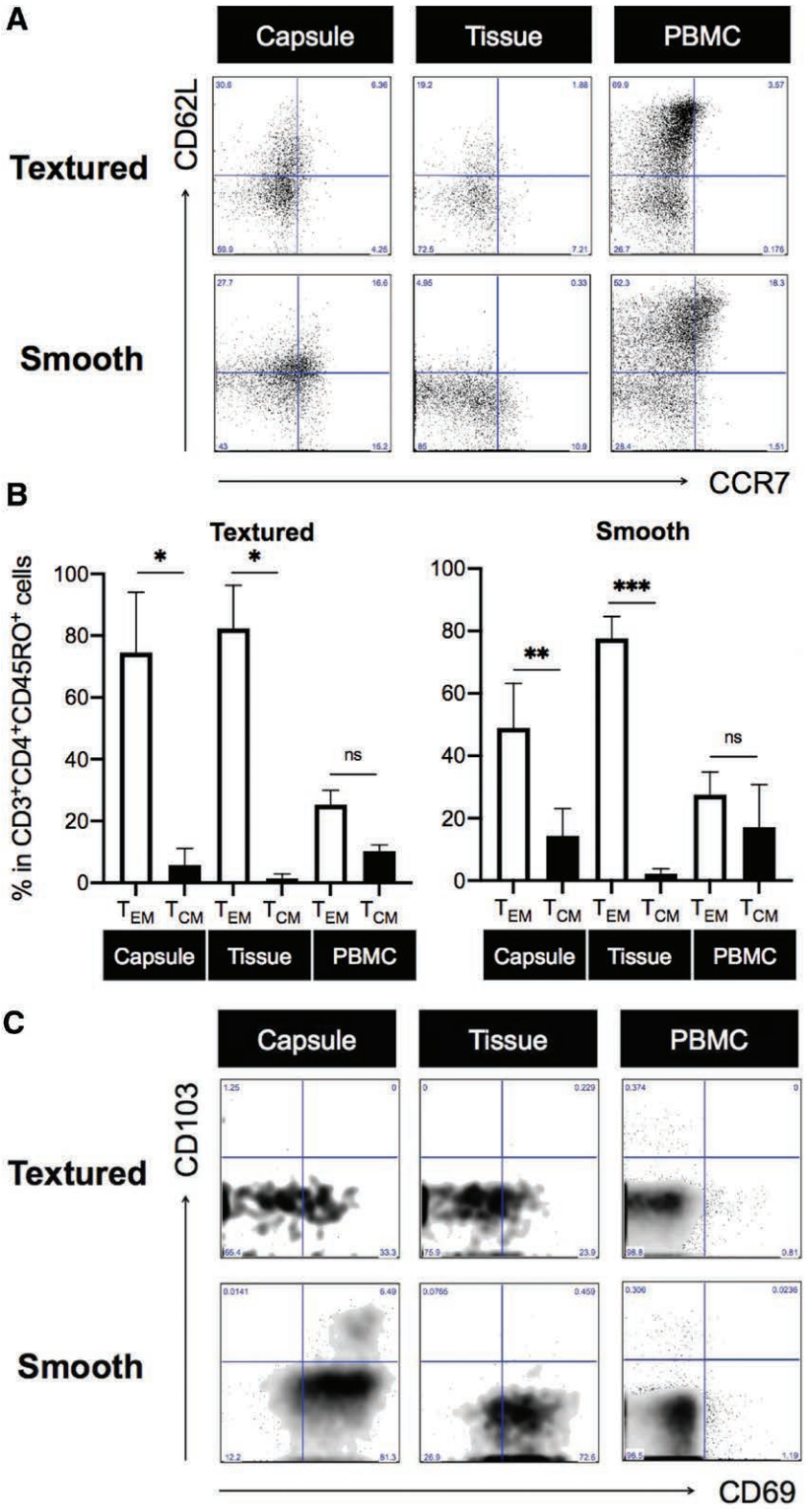


**Fig. 8.** A, Representative CD62L and CCR7 expression in the $CD3^+CD4^+$ T cells of indicated samples from textured and smooth TEs. B, A summary of CCR7 and CD62L expression from three different donors. C, Representative CD69 and CD103 expression in the $CD3^+CD4^+$ T cells of the indicated samples from textured and smooth TEs.

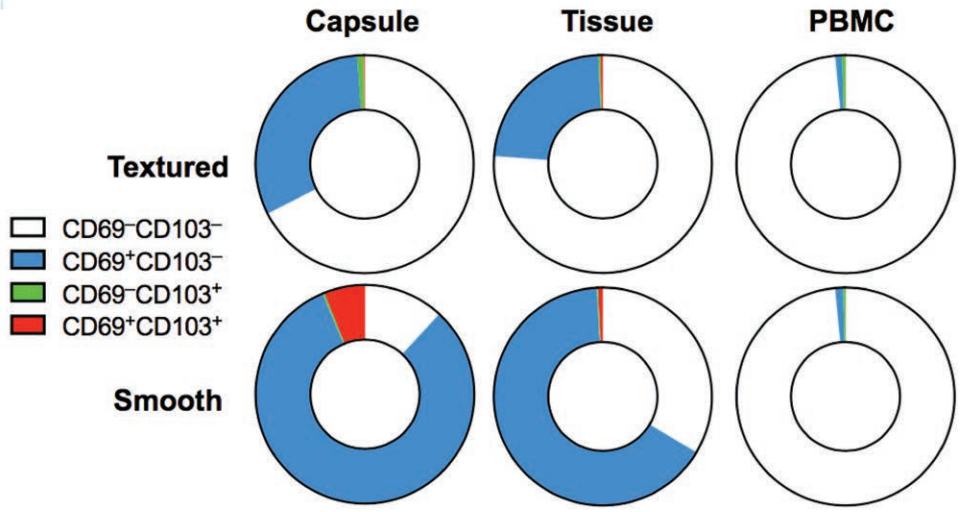


**Fig. 9.** A summary of CD69 and CD103 expression from three different donors.

**Statistical Analysis**

Statistical analysis was conducted using the Student *t* test (one-tailed). Differences of $*P < 0.05$, $**P < 0.01$, and $***P < 0.001$ were considered statistically significant.

## RESULTS

**Patient Demographic Data**

In this study, 19 female patients with a mean age of 49.94 years were enrolled. (**See table, Supplemental Digital Content 1, http://links.lww.com/PRSGO/B947.**) Mean body mass index was 21.35. Except for one patient who received bilateral reconstruction, all patients received unilateral reconstruction. All textured TE was Natrelle 133 (Allergan, Inc., Dublin, Ireland). As for smooth TE, Natrelle 133S (Allergan, Inc., Dublin, Ireland) and Integra (PMT corp., Chanhassen, USA) were used in three and two cases, respectively. In all patients, TEs were placed in the subpectoral layer. Acellular dermal matrix or any artificial materials were not used in any cases.

**Effector Memory CD4⁺ T Cells Are Predominant T-cell Infiltrate in the Capsule of Textured and Smooth TEs**

We obtained capsules and tissues adjacent to TE from both the textured and smooth TEs by thoroughly trimming subcutaneous fat. As observed previously, both the capsules and pericapsule tissues from smooth TE trended thicker than those from textured TE (Fig. 1). We also obtained peripheral blood mononuclear cells from the same donors. Capsules and tissues were enzymatically digested with a combination of collagenase type IV and DNase I to obtain single-cell suspensions. A small but evident population of CD3⁺ T-cell infiltrate was observed in both the capsules and tissues of both types of TE (Figs. 2, 3). CD3⁺ T cells consisted of CD4⁺ and CD8⁺ T cells, and CD4⁺ T cells were significantly dominant compared with CD8⁺ T cells in both the capsules and tissues from the two types of TE (Figs. 4, 5). Breast-implant–associated anaplastic large-cell lymphoma (BIA-ALCL) was primarily derived from CD4⁺ T cells. Approximately 80% of capsule- and tissue-infiltrating CD4⁺ T cells from both types of TE expressed CD45RO, suggestive of their memory phenotype (Fig. 6). CD45RO expression was significantly higher in CD4⁺ T cells than in CD8⁺ T cells (Fig. 7). In these capsule- and tissue-infiltrating memory CD4⁺ T cells, CCR7⁻CD62L⁻ effector memory CD4⁺ T cells were significantly greater than CCR7⁺CD62L⁺ central memory CD4⁺ T cells in the capsules and tissues from both types of TE (Fig. 8). These data indicate that effector memory CD4⁺ T cells predominantly infiltrate capsules and tissues without apparent differences between textured and smooth TE.

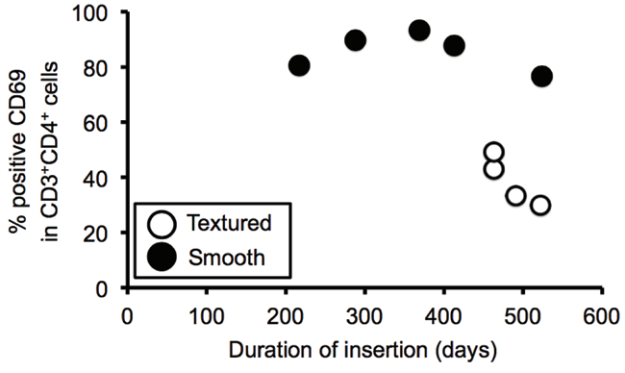


**Fig. 10.** The relation between duration of TE insertion and CD69 positivity in the CD3⁺CD4⁺ T cells.

**CD4⁺ Resident Memory T Cells are Generated by Smooth TE Rather than Textured TE**

We hypothesized that some capsule-infiltrating effector memory CD4⁺ T cells differentiate into resident memory T ($T_{RM}$) cells, which are a new entity of memory T cells that reside for a long time in a series of peripheral tissues, such as the skin, gut, and lungs, and that these $T_{RM}$ cells could be a progenitor of BIA-ALCL. In humans, $T_{RM}$ cells are defined as CD69-expressing T cells with or without CD103 expression. CD69⁺CD103⁺ T cells are definitively $T_{RM}$ cells, whereas CD69⁺CD103⁻ T cells are either $T_{RM}$ cells or activated T cells, because CD69 is one of the T-cell activation markers. Although we expected that $T_{RM}$ cells were

greater in the textured TE, $CD69^+CD103^+CD4^+$ T cells and $CD69^+CD103^-CD4^+$ T cells were greater in the capsules and tissues of smooth TE than in those of textured TE (Figs. 8, 9). Additionally, $CD4^+$ T cells infiltrated in the capsule of smooth TE exhibited higher CD69 expression irrespective of duration of TE insertion than those of textured TE (Fig. 10). Contrary to our hypothesis, these data suggest that $CD4^+$ $T_{RM}$ cells are generated by smooth TE and not by textured TE.

### *TNFRSF8/CD30* mRNA Expression is Higher in CD69-Null $CD4^+$ Effector Memory T Cells than CD69-Positive $CD4^+$ Effector Memory T Cells in the Textured TE

ALCL (including BIA-ALCL) is characterized by CD30 expression in lymphoma cells. Capsule- and tissue-infiltrating $CD4^+$ T cells from both types of TE did not express CD30 at the protein level (Fig. 11). However, in the capsule of textured TE, *TNFRSF8/CD30* mRNA expression was higher in the CD69-null capsule-infiltrating $CD4^+$ T cells than in the CD69-positive capsule-infiltrating $CD4^+$ T cells (Fig. 12).

## DISCUSSION

BIA-ALCL is currently defined as a textured breast-implant–associated CD30-positive and ALK-negative T-cell lymphoma. It was recently reported that chromosome 20q loss characterizes BIA-ALCL and distinguishes it from other types of ALCL, such as systemic ALK-positive ALCL ($ALK^+$ sALCL), ALK-negative ALCL ($ALK^-$ sALCL), and primary cutaneous ALCL (pcALCL), supporting the notion that BIA-ALCL is a discrete entity from $ALK^-$ sALCL and pcALCL.[10,11]

The pathophysiology of BIA-ALCL is much less understood than other types of ALCL. However, in the other three aforementioned types of ALCL devoid of BIA-ALCL, the origin of lymphoma cells is still not fully determined.[12] Nevertheless, T cells are currently presumed as the origin of ALCL due to the detection of T-cell receptor gene rearrangements. ALCL often exhibits loss of CD3, commonly expresses CD4, and rarely express CD8.[13–15] Consistent with this expression pattern, $CD4^+$ T cells were significantly predominant over $CD8^+$ T cells in the capsules from both types of TE.

Among cutaneous T-cell lymphoma (CTCL), lymphoma cells of Sezary syndrome (leukemic CTCL variants) are derived from central memory T ($T_{CM}$) cells, whereas those of mycosis fungoides (primarily cutaneous CTCL variants) are derived from resident memory T ($T_{RM}$) cells.[16–19] Moreover, BIA-ALCL and pcALCL have similar transcriptional and cytokine signatures.[20–22] Accordingly, we hypothesized that non-systemic, localized cutaneous lymphoma such as BIA-ALCL and pcALCL may originate from $CD4^+$ $T_{RM}$ cells like mycosis fungoides. The pathobiology of $T_{RM}$ cells remains unknown, particularly in humans. However, some effector memory T cells are observed to differentiate into $T_{RM}$ cells in response to local environmental stimuli in peripheral tissues, including the skin.[23] To support this notion, capsule-infiltrating $CD4^+$ T

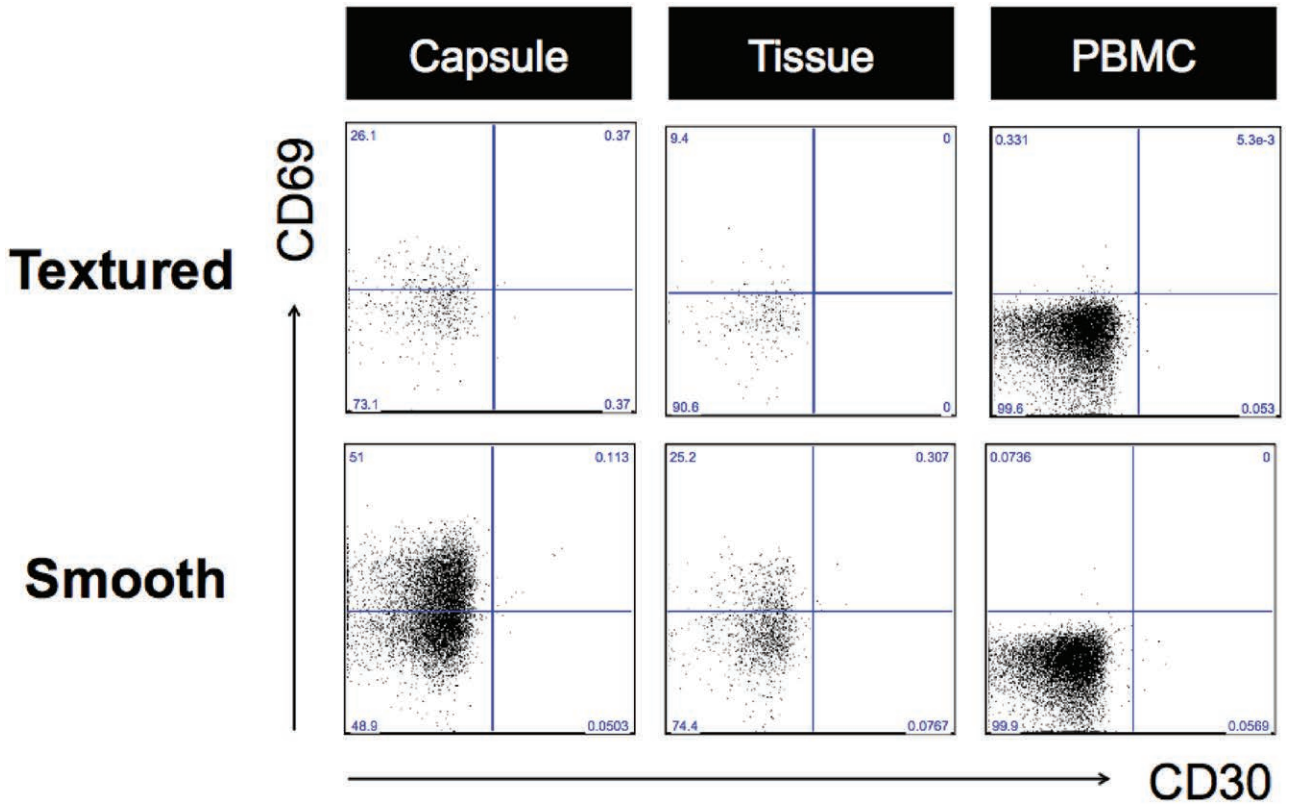


**Fig. 11.** Representative CD30 and CD69 expression in the $CD3^+CD4^+$ T cells of the indicated samples from textured and smooth TEs.

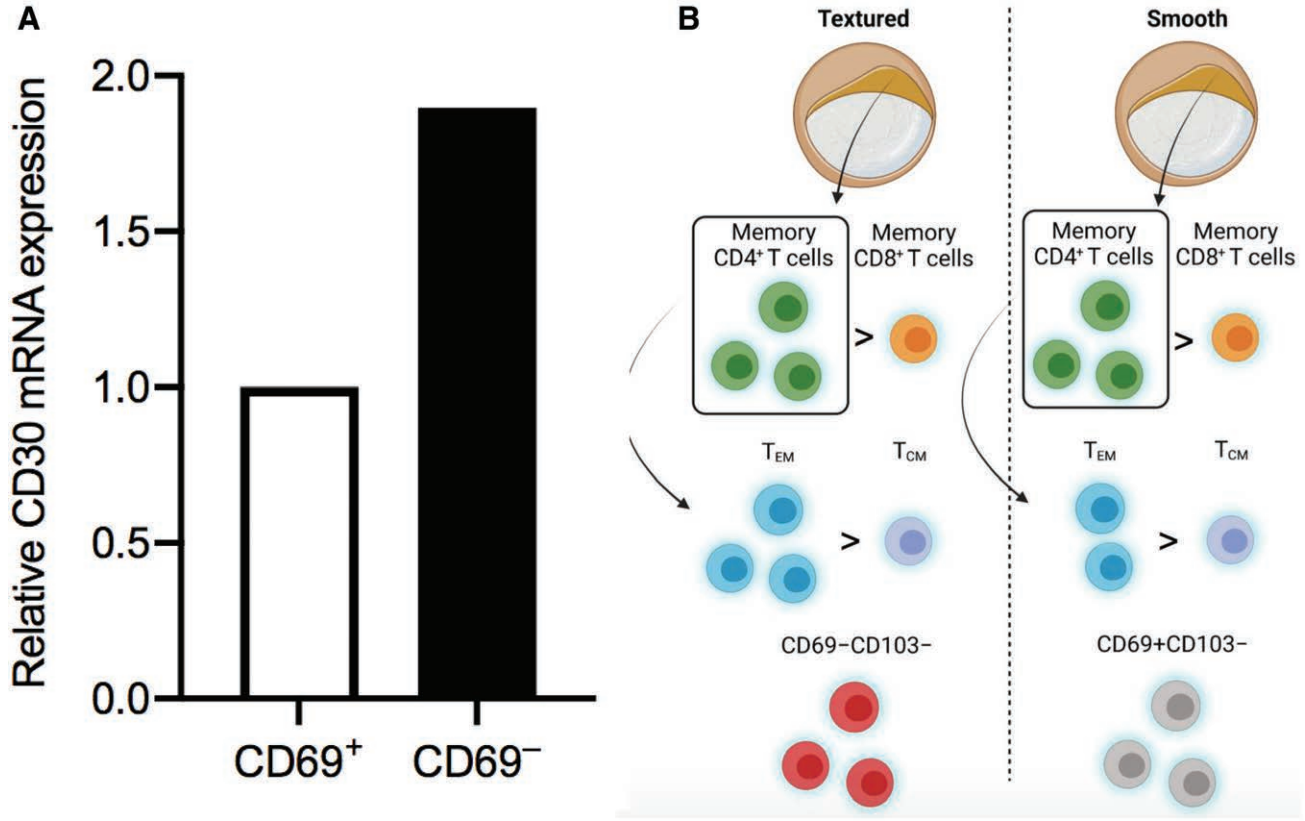


**Fig. 12.** A, Relative *TNFRSF8/CD30* mRNA expression of $CD3^+CD4^+CD69^-$ and $CD3^+CD4^+CD69^+$ T cells that were pooled from five capsules of textured-TE donors. B, Graphical abstract. In both textured and smooth capsules, memory $CD4^+$ T cells were greater than memory $CD8^+$ T cells. In memory $CD4^+$ T cells, effector memory T cells were greater than central memory T cells, suggesting that effector memory $CD4^+$ T cells were predominant T cells in the capsules. However, a phenotypic difference was observed between textured and smooth implants. Most of effector memory $CD4^+$ T cells in textured capsule were $CD69^-CD103^-$ cells, whereas those in smooth capsule were $CD69^+CD103^-$ cells. Collectively, $CD69^-$ effector memory $CD4^+$ T cells may be a possible origin of BIA-ALCL.

cells from both types of TE exhibited an effector memory phenotype. However, $CD4^+$ $T_{RM}$ cells were apparently enriched in the capsule of smooth, but not of textured, TE. The underlying mechanism by which smooth TE promotes $CD4^+$ $T_{RM}$-cell generation is unknown. In any case, given that BIA-ALCL is associated with textured implants but not with smooth implants, $CD4^+$ $T_{RM}$ cells as the origin of BIA-ALCL cells appears less feasible. CD30 expression is a hallmark of ALCL, including BIA-ALCL. We could not detect CD30 protein in the capsule-infiltrating $CD4^+$ T cells from both types of TE. We reasoned that the origin of BIA-ALCL cells at the least requires *TNFRSF8/CD30* mRNA. *TNFRSF8/CD30* mRNA expression was greater in the CD69-null capsule-infiltrating $CD4^+$ T cells than in the CD69-positive capsule-infiltrating $CD4^+$ T cells in the textured TE, supporting the idea that $CD4^+$ $T_{RM}$ cells ($CD69^+CD103^+$ or $CD69^+CD103^-$) are not the origin of BIA-ALCL cells.

A limitation of this study is a relatively short duration of TE insertion. We analyzed capsules derived from patients who had TE inserted a maximum of 600 days previously. Given that BIA-ALCL developed about 9 years, on average, following a textured breast-implant insertion,[9] significant events critical for BIA-ALCL development may occur at a later point. Additionally, we could not conduct transcriptome analysis using BIA-ALCL cells. Thus, the association between our findings and BIA-ALCL pathogenesis was not directly confirmed.

In conclusion, we propose that textured-implant–associated $CD69^-$ effector memory $CD4^+$ T cells that are exposed to chronic and continuous inflammatory stimuli elicited by the implant and/or pathogens may activate Janus kinase-STAT and oncogene drivers under hypoxic conditions, followed by the development of monoclonal, CD30-positive BIA-ALCL cells.[24–26]

## SUMMARY

Our current study demonstrates that effector memory $CD4^+$ T cells predominantly infiltrate capsules and tissues without apparent differences between textured and smooth TE. In these effector memory $CD4^+$ T cells, $CD4^+$ resident memory T ($T_{RM}$) cells are rather generated by smooth TE but not by textured TE. However, *TNFRSF8/CD30* mRNA expression is higher in the $CD69^-$ effector memory $CD4^+$ T cells compared with that in $CD69^+$ ones. Collectively, these data suggest that $CD69^+CD4^+$ $T_{RM}$ cells and/or activated $CD4^+$ T cells are not the origin of BIA-ALCL cells. Conversely, $CD69^-CD4^+$ effector memory T cells may be a possible

origin of BIA-ALCL cells (Fig. 12). (**See Video [online],** which displays how the generation of BIA-ALCL is associated with textured implants.)

***Youichi Ogawa, MD, PhD***
Department of Dermatology, Faculty of Medicine
University of Yamanashi
1110 Shimokato, Chuo
Yamanashi 409-3898
Japan
E-mail: yogawa@yamanashi.ac.jp

## ACKNOWLEDGEMENT

*We thank Dr. Naoki Oishi for his critical suggestion and review of the early draft of this article.*

## REFERENCES

1. Keech JA Jr, Creech BJ. Anaplastic T-cell lymphoma in proximity to a saline-filled breast implant. *Plast Reconstr Surg.* 1997;100:554–555.
2. Swerdlow SH, Campo E, Pileri SA, et al. The 2016 revision of the World Health Organization classification of lymphoid neoplasms. *Blood.* 2016;127:2375–2390.
3. Collett DJ, Rakhorst H, Lennox P, et al. Current risk estimate of breast implant-associated anaplastic large cell lymphoma in textured breast implants. *Plast Reconstr Surg.* 2019;143:30S–40S.
4. Clemens MW, Jacobsen ED, Horwitz SM. 2019 NCCN consensus guidelines on the diagnosis and treatment of breast implant-associated anaplastic large cell lymphoma (BIA-ALCL). *Aesthet Surg J.* 2019;39(suppl_1):S3–S13.
5. US Food and Drug Administration. The FDA requests Allergan voluntarily recall Natrelle BIOCELL textured breast implants and tissue expanders from the market to protect patients: FDA safety communication. June 1, 2020. Available at https:// www.fda.gov/medical-devices/safety-communications/fdarequests-allergan-voluntarily-recall-natrelle-biocell-texturedbreast-implants-and-tissue. Accessed September 28, 2020.
6. Barone FE, Perry L, Keller T, et al. The biomechanical and histopathologic effects of surface texturing with silicone and polyurethane in tissue implantation and expansion. *Plast Reconstr Surg.* 1992;90:77–86.
7. Maxwell GP, Van Natta BW, Bengtson BP, et al. Ten-year results from the Natrelle 410 anatomical form-stable silicone breast implant core study. *Aesthet Surg J.* 2015;35:145–155.
8. Danino AM, Basmacioglu P, Saito S, et al. Comparison of the capsular response to the Biocell RTV and Mentor 1600 Siltex breast implant surface texturing: a scanning electron microscopic study. *Plast Reconstr Surg.* 2001;108:2047–2052.
9. Turner SD, Inghirami G, Miranda RN, et al. Cell of origin and immunologic events in the pathogenesis of breast implant-associated anaplastic large-cell lymphoma. *Am J Pathol.* 2020;190:2–10.
10. de Leval L. Chromosomes in breast lymphoma. *Blood.* 2020;136:2848–2849.
11. Los-de Vries GT, de Boer M, van Dijk E, et al. Chromosome 20 loss is characteristic of breast implant-associated anaplastic large cell lymphoma. *Blood.* 2020;136:2927-2932.
12. Eckerle S, Brune V, Döring C, et al. Gene expression profiling of isolated tumour cells from anaplastic large cell lymphomas: insights into its cellular origin, pathogenesis and relation to Hodgkin lymphoma. *Leukemia.* 2009;23:2129–2138.
13. Lechner MG, Megiel C, Church CH, et al. Survival signals and targets for therapy in breast implant-associated ALK–anaplastic large cell lymphoma. *Clin Cancer Res.* 2012;18:4549–4559.
14. Juco J, Holden JT, Mann KP, et al. Immunophenotypic analysis of anaplastic large cell lymphoma by flow cytometry. *Am J Clin Pathol.* 2003;119:205–212.
15. Kesler MV, Paranjape GS, Asplund SL, et al. Anaplastic large cell lymphoma: a flow cytometric analysis of 29 cases. *Am J Clin Pathol.* 2007;128:314–322.
16. Campbell JJ, Clark RA, Watanabe R, et al. Sezary syndrome and mycosis fungoides arise from distinct T-cell subsets: a biologic rationale for their distinct clinical behaviors. *Blood.* 2010;116:767–771.
17. Kirsch IR, Watanabe R, O'Malley JT, et al. TCR sequencing facilitates diagnosis and identifies mature T cells as the cell of origin in CTCL. *Sci Transl Med.* 2015;7:308ra158.
18. Clark RA, Watanabe R, Teague JE, et al. Skin effector memory T cells do not recirculate and provide immune protection in alemtuzumab-treated CTCL patients. *Sci Transl Med.* 2012;4:117ra7.
19. Watanabe R. Protective and pathogenic roles of resident memory T cells in human skin disorders. *J Dermatol Sci.* 2019;95:2–7.
20. Kadin ME, Deva A, Xu H, et al. Biomarkers provide clues to early events in the pathogenesis of breast implant-associated anaplastic large cell lymphoma. *Aesthet Surg J.* 2016;36:773–781.
21. Laimer D, Dolznig H, Kollmann K, et al. PDGFR blockade is a rational and effective therapy for NPM-ALK-driven lymphomas. *Nat Med.* 2012;18:1699–1704.
22. Schiefer AI, Vesely P, Hassler MR, et al. The role of AP-1 and epigenetics in ALCL. *Front Biosci (Schol Ed).* 2015;7:226–235.
23. Clark RA. Resident memory T cells in human health and disease. *Sci Transl Med.* 2015;7:269rv1.
24. Oishi N, Brody GS, Ketterling RP, et al. Genetic subtyping of breast implant-associated anaplastic large cell lymphoma. *Blood.* 2018;132:544–547.
25. Oishi N, Miranda RN, Feldman AL. Genetics of breast implant-associated anaplastic large cell lymphoma (BIA-ALCL). *Aesthet Surg J.* 2019;39(suppl_1):S14–S20.
26. Oishi N, Hundal T, Phillips JL, et al. Molecular profiling reveals a hypoxia signature in breast implant-associated anaplastic large cell lymphoma. *Haematologica.* 2021;106:1714–1724.